

## Triclinic feldspars: angular relations and the representation of feldspar series

JAMES B. THOMPSON, JR.

*Department of Geological Sciences, Harvard University  
Cambridge, Massachusetts 02138*

AND GUY L. HOVIS

*Department of Geology, Lafayette College  
Easton, Pennsylvania 18042*

### Abstract

The rhombic section angles and obliquities of triclinic feldspars are simple trigonometric functions of  $\alpha^*$  and  $\gamma$ . Alkali-exchange series and short-term heating experiments show wide variation in  $\alpha^*$  but little variation in  $\gamma$ . Differing degrees of Al–Si order at constant composition and temperature cause wide variations in  $\gamma$  and relatively minor ones in  $\alpha^*$ . Graphical methods are developed by which  $\alpha^*$ ,  $\gamma$ , rhombic section angle, and obliquity can be read easily from a single plot. The same plot also differentiates the various types of feldspar series at least as well as any other in current use.

The obliquity,  $\phi$ , is a direct measure of the departure of a triclinic feldspar from the dimensional requirements for monoclinic symmetry. The quantity  $(1 - \cos\phi)$  must vanish for monoclinic feldspars and is a nearly linear function of temperature for isochemical feldspar series that approach a monoclinic state on heating. A new convention is proposed for defining the rhombic section of potassic feldspars in order to make their values consistent with those of contiguous K–Na feldspars.

Feldspars of a given composition that are in full internal equilibrium should lie along unique paths in terms of  $\alpha^*$  and  $\gamma$ . Sufficient information is now at hand to show the general form of such paths for K–Na–Ca feldspars, and to provide preliminary formulations of these paths for the end-member feldspars.

### Introduction

The idealized structure of feldspar is topologically consistent with monoclinic symmetry, and certain potassium and barium feldspars are indeed monoclinic. The most abundant feldspars in rocks, however, are triclinic, but even in these the departures of lattice parameters from the requirements for monoclinic symmetry are small. Many such feldspars can be transformed continuously into monoclinic forms, either by heat treatment or by alkali exchange.

Departures of a triclinic crystal from the dimensional requirements of monoclinic symmetry may be described completely in terms of two independent angular measurements. With the  $b$ -axis chosen (in the triclinic crystals) to correspond topologically to the  $b$ -axis of a possible monoclinic variant, a sufficient pair would be either the  $\alpha$  and  $\gamma$  angles of the direct cell, or the  $\alpha^*$  and  $\gamma^*$  angles of the reciprocal cell. Pairs such as  $\alpha^*$  and  $\gamma$ , or  $\alpha$  and  $\gamma^*$ , however, will also

suffice, although it may seem aesthetically unappealing, at first, to mix direct and reciprocal quantities. If  $\alpha^*$  and  $\gamma$  or  $\alpha$  and  $\gamma^*$  are chosen, mathematical and trigonometric advantages are gained (see later discussion), since angles are determined by axial elements that lie in two mutually orthogonal planes. This is not generally true if both angles selected are direct or both reciprocal.

We shall show that  $\alpha^*$  [which also may be regarded as the dihedral angle between the (001) and (010) cleavages] and  $\gamma$  [which is a measure of the obliquity of the (001) face of the unit cell] provide unique advantages in the treatment of triclinic feldspars. *Other angles of special interest are related to them by simple trigonometric equations, much more simple ones, in fact, than the ones obtaining if wholly direct or wholly reciprocal cell-angles are used.* Changes brought about by short-term heating, or by short-term alkali exchange, cause wide variations in  $\alpha^*$

with but slight variations in  $\gamma$  (nearly negligible, in fact, in many instances). The effects of long-term heating, in feldspars as subsequently examined at room temperature, cause wide variations in  $\gamma$  and relatively minor variations in  $\alpha^*$ . Although we are concerned primarily with triclinic feldspars, many of the methods developed are applicable to any mineral group containing triclinic crystals that show continuous variations about a monoclinic limit.

### Obliquity

In a monoclinic crystal, conventionally oriented, it is necessary (but not sufficient) that the  $b$ -axis and the pole,  $b^*$ , to (010) coincide, and that  $b = 1/b^* = d(010)$ . In a triclinic crystal, on the other hand,  $b$  and  $b^*$  do not, in general, coincide. We shall therefore follow Donnay (1940) and designate the angle,  $\phi$ , between them as the *obliquity*. It follows that

$$d(010) = 1/b^* = b \cos\phi \quad (1)$$

Inasmuch as the cell volume,  $V_c$ , of a monoclinic crystal is  $abc \sin\beta$ , that for a triclinic crystal is given by

$$V_c = abc \sin\beta \cos\phi \quad (2)$$

Similarly for the reciprocal cell volume  $V_c^*$

$$V_c^* = a^*b^*c^* \sin\beta^* \cos\phi \quad (3)$$

Although it is necessary for monoclinic symmetry that  $\phi = 0$  or  $\cos\phi = 1$ , it is possible (though we know of no examples) that a triclinic crystal may also have zero obliquity, despite the origin of the word "triclinic". The vanishing of the obliquity thus insures only that the *geometric form* of the unit cell meets the requirements for monoclinic symmetry, and does not prove that the crystal is indeed monoclinic. Such a crystal, for example, might have an Al-Si distribution that is inconsistent with monoclinic symmetry.

The obliquity as used here, in the sense of Donnay, should not be confused with the quantity [ $d(1\bar{3}1) - d(131)$ ] which has been called the "triclinicity" by Goldsmith and Laves (1954) and "obliquity" by McConnell and McKie (1960; see also Martin, 1969, 1970). Although the quantity [ $d(1\bar{3}1) - d(131)$ ] must vanish when  $\phi$  vanishes, the reverse is not true. The vanishing of  $\phi$  is thus the more stringent requirement for monoclinic symmetry, though not in itself sufficient.

### Rhombic section

The *rhombic section* (Rath, 1876) of a triclinic feldspar is defined, traditionally, as the section contain-

ing  $b$  on which the traces of the forms (110) and ( $\bar{1}\bar{1}0$ ) form a rhombus. Inasmuch as the diagonals of a rhombus intersect at right angles, an alternative and more practical definition is to define the rhombic section as the plane defined by  $b$  and the line  $r$  in (010) that is perpendicular to  $b$ . As a section of the unit cell the rhombic section is thus a *rectangular section*, which might indeed be a better name for it. If  $\phi \neq 0$  there is a unique rhombic or rectangular section, but if  $\phi = 0$ , all sections containing  $b$  are rhombic sections and *the* rhombic section, as a unique plane, is indeterminate. Even in this last instance, however, we may have interest in a *limiting rhombic section* when dealing with a phase transformation in which  $\phi \rightarrow 0$  continuously. The orientation of the rhombic section may be specified in two alternate ways: either as the dihedral angle, which we shall designate as  $\sigma^*$ , between the rhombic section and (001); or by the angle  $\sigma$ , between  $r$  and  $a$ , which is thus an angle in (010). Feldspars have low obliquities (less than  $5^\circ$ ), hence the distinction between  $\sigma$  and  $\sigma^*$  is of little practical importance and does not exceed a few hundredths of a degree at most.

We shall find it useful to designate the line normal to  $r$  in (010) as  $s$ , and the pole to the rhombic section as  $s^*$ ;  $r$  is thus normal to  $s$ ,  $s^*$ ,  $b$  and  $b^*$ . In addition  $b$  is normal to  $s^*$ ,  $c^*$  or  $a^*$ , and  $b^*$  to  $s$ ,  $a$  or  $c$ , hence

$$s \wedge s^* = b \wedge b^* \equiv \phi \quad (4)$$

Also

$$r \wedge a \equiv \sigma = s \wedge [\perp a \text{ in } (010)] \quad (5)$$

$$s^* \wedge c^* \equiv \sigma^* = r \wedge [\perp b \text{ in } (001)] \quad (6)$$

as shown in Figure 1. If  $\phi \neq 0$  in a triclinic feldspar and  $\gamma$  is  $90^\circ$ , the rhombic section must coincide with (001); and if  $\alpha^*$ , which is also the angle between the (010) and (001) cleavages, is  $90^\circ$ , the rhombic section must be normal to (001). In each of these special cases  $\sigma$  and  $\sigma^*$  are identical.

### Orientation of triclinic feldspars

The crystallographic reference axes for triclinic feldspars are chosen so as to correspond topologically to those of monoclinic feldspars. In centrosymmetric monoclinic feldspars, because the axes are non-polar, there are two entirely equivalent ways of selecting the positive ends of these axes so as to form a right-handed array. In centrosymmetric triclinic feldspars, though the axes are still non-polar, the corresponding two ways are non-equivalent. An early convention was to choose the orientation that made

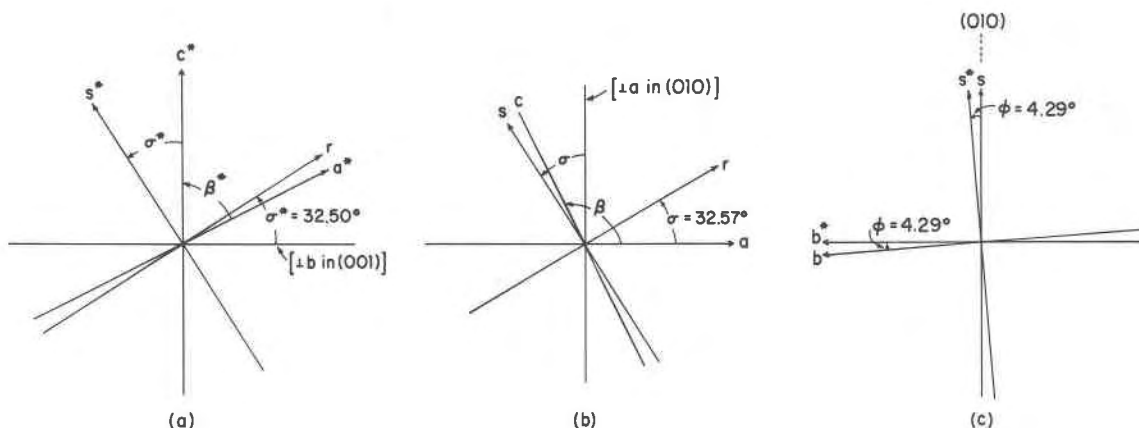


Fig. 1. Angular relationships in Amelia albite (F101 of Grundy and Brown, 1969). (a) Axial elements normal to  $b^*$  as viewed in positive direction along  $b$ . (b) Axial elements normal to  $b^*$  as viewed in positive direction along  $b^*$ . (c) Axial elements normal to  $r$  as viewed in positive direction along  $r$ . The crystal is in conventional orientation ( $\alpha$  obtuse). Arrows show positive ends of axes.

$\alpha^*$  acute, but Laves (1951) demonstrated that this orientation placed microclines out of proper context relative to other closely-related triclinic feldspars and proposed a new convention such that  $\alpha$  for all triclinic feldspars be taken as obtuse. We shall refer herein to the latter orientation as *conventional*, and to the orientation of feldspars so that  $\alpha$  is acute as *anti-conventional*. The principal ambiguities that arise are with K-rich triclinic feldspars of very low obliquity such that the departure of  $\alpha$  from  $90^\circ$  lies within the experimental error. If this occurs, the orientation is consistent with those for related feldspars if  $\gamma$  is taken as acute. Grove and Hazen (1974), for example, give  $\alpha = 90^\circ$  and  $\gamma = 90.07^\circ$  for an adularia at the temperature of liquid nitrogen. This results in the anti-conventional orientation; the conventional one would have  $\gamma = 89.93^\circ$ .

The distinction between conventional and anti-conventional orientations is useful (see Thompson *et al.*, 1974) in dealing with ordering, with twinning, and with domain structures as related to monoclinic-triclinic transformations. A change from the one orientation to the other may be effected by interchanging the positive and negative ends of  $a$ ,  $a^*$ ,  $c$  and  $c^*$ , but not of  $b$  or  $b^*$ . An immediate consequence of such a re-orientation is that *cosines* of  $\alpha$ ,  $\alpha^*$ ,  $\gamma$ , and  $\gamma^*$  all change sign (acute becomes obtuse and *vice versa*). Their *sines*, however, are unaffected. Angles such as  $\beta$  and  $\beta^*$  and their trigonometric functions, on the other hand, are entirely unchanged. Properties that change sign on reorientation are *odd-symmetric* in the sense of Thompson *et al.* (1974, p. 220–222); those that are entirely unaffected are *even-symmetric*.

The angular relations at  $25^\circ\text{C}$  for a typical low albite (F101 of Grundy and Brown, 1969) are shown in Figure 1 for the crystal in conventional orientation. The arrows indicate what we shall take as positive directions for  $r$ ,  $s$ , and  $s^*$ . In a K–Na exchange series from low albite to microcline,  $\sigma$  and  $\sigma^*$  increase continuously to between  $100^\circ$  and  $105^\circ$  as measured at  $250^\circ\text{C}$ , and a similar effect may be observed through short-term, reversible heating of low albite. Long-term heating of albite, however, reduces the values of  $\sigma$  and  $\sigma^*$  continuously to a limiting value of about  $-3^\circ$  if measured at room temperature after heat treatment. Calcic plagioclases have still lower values of  $\sigma$  and  $\sigma^*$ , to between  $-15^\circ$  and  $-20^\circ$  for pure anorthite. For all of these feldspars the appearance of Figure 1c remains much the same, despite the wide variations in  $\sigma$  and  $\sigma^*$ .

For feldspars placed in anti-conventional orientations, the positive and negative ends of the  $a$ ,  $a^*$ ,  $c$ , and  $c^*$  axes are interchanged. The positive ends of  $b$  and  $b^*$ , however, remain as before. We shall find it convenient to take  $\phi$  as always positive, and thus to permit the positive ends of  $r$ ,  $s$ , and  $s^*$  to rotate with the crystal during its re-orientation. The  $\sigma$  and  $\sigma^*$  values for crystals in anti-conventional orientation will then be the supplements of the values for the same crystal in conventional orientation, so that  $\sigma$  or  $\sigma^*$  anti-conventional = ( $\sigma$  or  $\sigma^*$  conventional  $- 180^\circ$ ). This results in values ranging from about  $-80^\circ$  in microcline to about  $-195^\circ$  in anorthite when placed in anti-conventional orientation.

The angles given in the above two paragraphs are at variance with the tradition that  $\sigma$  or  $\sigma^*$  always be

reported as acute angles, but we shall see that the system used here leads to a simpler trigonometric treatment and to a simpler graphical presentation thereof. It will also prevent the  $\sigma$  and  $\sigma^*$  values for low albite-microcline exchange series from undergoing a  $180^\circ$  discontinuity near the K-end of the series! The revisions indicated above are thus entirely consistent with, and an extension of, the revised orientation introduced by Laves (1951), and also make use of the obliquity as defined by Donnay (1940).

### Trigonometric relations

Either  $r$ ,  $b$ , and  $s^*$  or  $r$ ,  $b^*$ , and  $s$  may be taken as a set of mutually orthogonal reference axes for obtaining the desired trigonometric equations relating rhombic section angles and obliquity to the standard axial angles of crystallography. The results using either set are identical, hence we shall show the derivation only for one. In terms of  $r$ ,  $b$ , and  $s^*$  the direction cosines of other axes of interest are given in Table 1 (compare with Fig. 1). With the aid of Table 1 we then obtain the following

$$\begin{aligned} \cos(a \wedge b^*) &= 0 \\ &= \cos\phi \cos\gamma + \sin\phi \cos(a \wedge s^*) \end{aligned} \quad (7)$$

$$\begin{aligned} \cos(a \wedge c^*) &= 0 \\ &= \cos\sigma \sin\sigma^* + \cos\sigma^* \cos(a \wedge s^*) \end{aligned} \quad (8)$$

$$\begin{aligned} \cos(a \wedge s) &= -\sin\sigma \\ &= -\sin\phi \cos\gamma + \cos\phi \cos(a \wedge s^*) \end{aligned} \quad (9)$$

And, because  $b^* \wedge c^* = \alpha^*$ , we also have

$$\cos\alpha^* = \sin\phi \cos\sigma^* \quad (10)$$

Eliminating  $\cos(a \wedge s^*)$  from (7) and (9) we obtain

$$\cos\gamma = \sin\phi \sin\sigma \quad (11)$$

and eliminating both  $\cos\gamma$  and  $\cos(a \wedge s^*)$  from (7), (8), and (9) we obtain

$$\cos\phi = \tan\sigma^*/\tan\sigma \quad (12)$$

By squaring both sides of (10) and (12) we may eliminate functions of  $\phi$ . Because we have defined  $\sigma$  and  $\sigma^*$  so that all their trigonometric functions have the same sign (and even the same magnitude when either  $\alpha^*$  or  $\gamma$  is  $90^\circ$ ), and because  $\alpha^*$  (and also  $\gamma$ ) are always taken as positive angles less than  $180^\circ$ , we obtain

$$\sin\alpha^* = \sin\sigma^*/\sin\sigma \quad (13)$$

which has been derived by Lewis (1899). Squaring both sides of (11) and (12) and repeating the same procedure we have

$$\sin\gamma = \cos\sigma/\cos\sigma^* \quad (14)$$

The remaining equations of interest may all be obtained by simple algebraic manipulation. From (10), (12), and (13) we have

$$\cot\alpha^* = \tan\phi \cos\sigma \quad (15)$$

and from (11), (12), and (14)

$$\cot\gamma = \tan\phi \sin\sigma^* \quad (16)$$

and from (12), (13), and (14)

$$\cos\phi = \sin\alpha^* \sin\gamma \quad (17)$$

as obtained by Donnay (1940; see also Gay, 1956). Finally, combining (10) and (11) with (13) and (14), respectively, we obtain

$$\tan\sigma^* = \cos\gamma/\cot\alpha^* \quad (18)$$

and

$$\tan\sigma = \cot\gamma/\cos\alpha^* \quad (19)$$

Equation (18) has also been derived by Tunell (1952) and equation (19) by Story-Maskelyne (1895), Lewis (1899) and Mügge (1930; correcting an earlier version by Rosenbusch and Mügge, 1927; see also Tunell, 1952). Several of the others quite possibly appear elsewhere in the early crystallographic literature.

It is evident from equations (10) through (19) that no more than two of the five angles  $\alpha^*$ ,  $\gamma$ ,  $\phi$ ,  $\sigma$ , and  $\sigma^*$  may be taken as independent, and that these ten equations, in fact, relate all possible sets of three out of the five. Our choice of a reciprocal angle  $\alpha^*$  and a direct angle  $\gamma$  rather than  $\alpha$  and  $\gamma$  or  $\alpha^*$  and  $\gamma^*$  may be disturbing to a purist who prefers to keep direct things direct and reciprocal things reciprocal, but it has many advantages. Not least of these is that *for-*

Table 1. Direction cosines referred to  $r$ ,  $b$ , and  $s^*$  as reference axes

Line "L"	Cos LAr	Cos LAb	Cos LAs*
$r$	1	0	0
$b$	0	1	0
$s^*$	0	0	1
$b^*$	0	$\cos\phi$	$\sin\phi$
$s$	0	$-\sin\phi$	$\cos\phi$
$a$	$\cos\sigma$	$\cos\gamma$	$\cos(a\wedge s^*)$
$c^*$	$\sin\sigma^*$	0	$\cos\sigma^*$

mulas analogous to (10) through (19) wholly in terms of  $\alpha$  and  $\gamma$  or of  $\alpha^*$  and  $\gamma^*$  are much more cumbersome and require introduction of either  $\beta$  or  $\beta^*$ , respectively, which the above relations avoid.  $\alpha^*$  and  $\gamma$  (or  $\alpha$  and  $\gamma^*$  for that matter) also have the advantage of being angles lying in two mutually orthogonal planes ( $\alpha^*$  in the plane normal to  $a$ , and  $\gamma$  in the plane normal to  $c^*$ ).  $\alpha^*$  may also be identified with the angle of intersection of the (001) and (010) cleavages, and thus lends itself to direct measurement by several means, provided crystals are of sufficient size.

**Graphical relations between  $\alpha^*$  and  $\gamma$**

Figure 2a and Figure 2b are graphical representations of equations (18) and (19), respectively. They appear much the same, and even when superposed can be distinguished only if very carefully drawn. For a positive angle,  $\theta$ , near  $90^\circ$  we have, if  $\theta$  is in radians,

$$\cos\theta \leq (\pi/2 - \theta) \leq \cot\theta \quad (\theta \text{ acute}) \quad (20a)$$

$$\cos\theta \geq (\pi/2 - \theta) \geq \cot\theta \quad (\theta \text{ obtuse}) \quad (20b)$$

and all three quantities are very nearly the same. In feldspars neither  $\alpha^*$  nor  $\gamma$  departs from  $90^\circ$  by more than  $4.25^\circ$  (0.0742 radians), for which  $\cos\theta = 0.0741$  and  $\cot\theta = 0.0743$ . For angles closer to  $90^\circ$  the agreement is even better, and the three quantities become identical as  $\theta$  approaches  $90^\circ$ . Both diagrams also show clearly the distinction between the conventional and anti-conventional orientation for a given feldspar, as well as further justification for the revision suggested earlier in assigning numerical values to  $\sigma$  and  $\sigma^*$ . Figures 2a and 2b also correspond very closely to Figures 1a and 1b, respectively. In Figures 2a and 2b a line extending from the origin to a plotted point may be regarded as a vector corresponding to the axis  $r$  in Figure 1a or 1b. *The angle subtended by this vector and the positive x-axis is the corresponding rhombic section angle. There is also a close relationship between the magnitude of the vector  $r$  and that of the obliquity.* By squaring both sides of equation (17) we may obtain either

$$\cot^2\alpha^*/\tan^2\phi + \cos^2\gamma/\sin^2\phi = 1 \quad (21)$$

or

$$\cot^2\gamma/\tan^2\phi + \cos^2\alpha^*/\sin^2\phi = 1 \quad (22)$$

Equations (21) and (22) may be regarded as the equations of curves of constant obliquity in Figures 2a and 2b, respectively. Both are the equations of ellipses, centered at the origin, that are nearly circular. For a given value of  $\phi$  the two ellipses are con-

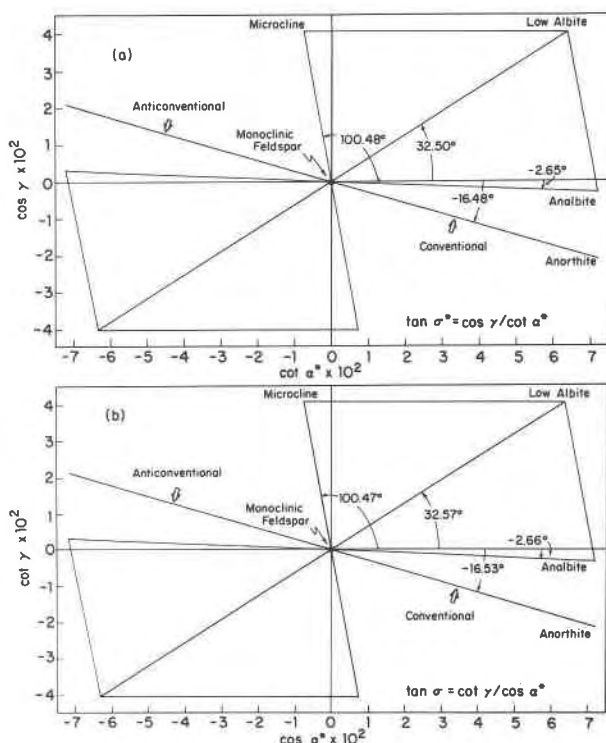


Fig. 2. Relations between  $\alpha^*$ ,  $\gamma$ ,  $\sigma$ ,  $\phi$ , and  $\sigma^*$  for: authigenic microcline (M-201-Nd, Kastner, 1971); low albite (F101, Grundy and Brown, 1969); analbite (307, Grundy and Brown, 1969); anorthite (Cole *et al.*, 1951); and sanidine. (a) corresponds to equation (18) and (b) to equation (19).

gruent, but the foci of the ellipse for Figure 2a are close to the origin on the x-axis, and the foci for the ellipse in Figure 2b are at the same distance from the origin on the y-axis. The coordinates of the foci in either case are  $\pm\sin\phi \tan\phi$ . The ellipses are nearly circular because  $\phi$  is a small positive angle ( $4.5^\circ$  or less). If  $\phi$  is in radians we have

$$\sin\phi \lesssim \phi \lesssim \tan\phi \quad (23)$$

and also, from either (21) or (22),

$$\sin\phi \lesssim r \lesssim \tan\phi \quad (24)$$

The four quantities  $\sin\phi$ ,  $\tan\phi$ ,  $r$ , and  $\phi$  (in radians) are thus virtually indistinguishable graphically from one another, and *we may take the length of the vector  $r$ , for a plotted feldspar in either Figure 2a or 2b, as the magnitude of  $\phi$  (in radians), very nearly.* Because Figure 2a shows (as does Fig. 1a) the rhombic section angle,  $\sigma^*$ , as measured in a section normal to  $b$ , the conventional and anti-conventional plots for a given feldspar in Figure 2a may be thought of as twins related by the pericline law. The corresponding plots

in Figure 2b may be thought of as twins related by the albite law.

It also follows from (20a,b) that a plot of  $(\pi/2-\gamma)$  against  $(\pi/2-\alpha^*)$ , both in radians, produces a diagram that is intermediate between Figure 2a and 2b, hence virtually indistinguishable from either. Equation (17), rewritten as

$$\cos\phi = \cos(\pi/2-\alpha^*) \cos(\pi/2-\gamma) \quad (25)$$

is the equation of a curve of constant obliquity on this third diagram, and is the equation of a nearly circular transcendental curve of fourfold ( $4mm$ ) symmetry. If the corresponding angles are plotted in degrees rather than radians, the diagram differs only by a scale factor, and the vector  $r$  is then very nearly equal in magnitude to  $\phi$  in degrees.

Other alternatives essentially equivalent to the above would be polar coordinate plots in terms of  $\sigma$ , or  $\sigma^*$ , and  $\phi$ , in either radians or degrees, as the radius vector. Whichever representation one chooses is a matter of aesthetics or whim and makes little practical difference. We shall see that *plots such as those suggested here provide not only a graphical display of obliquity and rhombic section angle, but also*

*differentiate the various feldspar series of interest at least as clearly as do the  $\alpha^*-\gamma^*$  plot of MacKenzie and Smith (1955) or the  $\alpha-\gamma$  plot of Orville (1967).* The paths of series of feldspars related to one another by displacive transformation or alkali exchange are, in fact, nearly orthogonal, in the plots here proposed, to those of series of feldspars related to one another by the diffusive redistribution of Al and Si.

### End-member feldspars

As observed at room temperature, the end-member K- and Na-feldspars show wide variation in  $\gamma$ , accompanied by relatively slight variation in  $\alpha^*$ . Ca-feldspars, on the other hand, show little or no variation in either  $\alpha^*$  or  $\gamma$ . The K- and Na-feldspars that have the most acute values of  $\gamma$  (when in conventional orientation) are those from low-temperature geologic environments. Prolonged heat treatment of such feldspars lowers  $\cos\gamma$  and converts these feldspars into forms like those from higher-temperature environments. The results obtained by Baskin (1956) through long-term heating of low-temperature microcline and albite are plotted in Figure 3. Structural studies have shown that the low-temperature forms

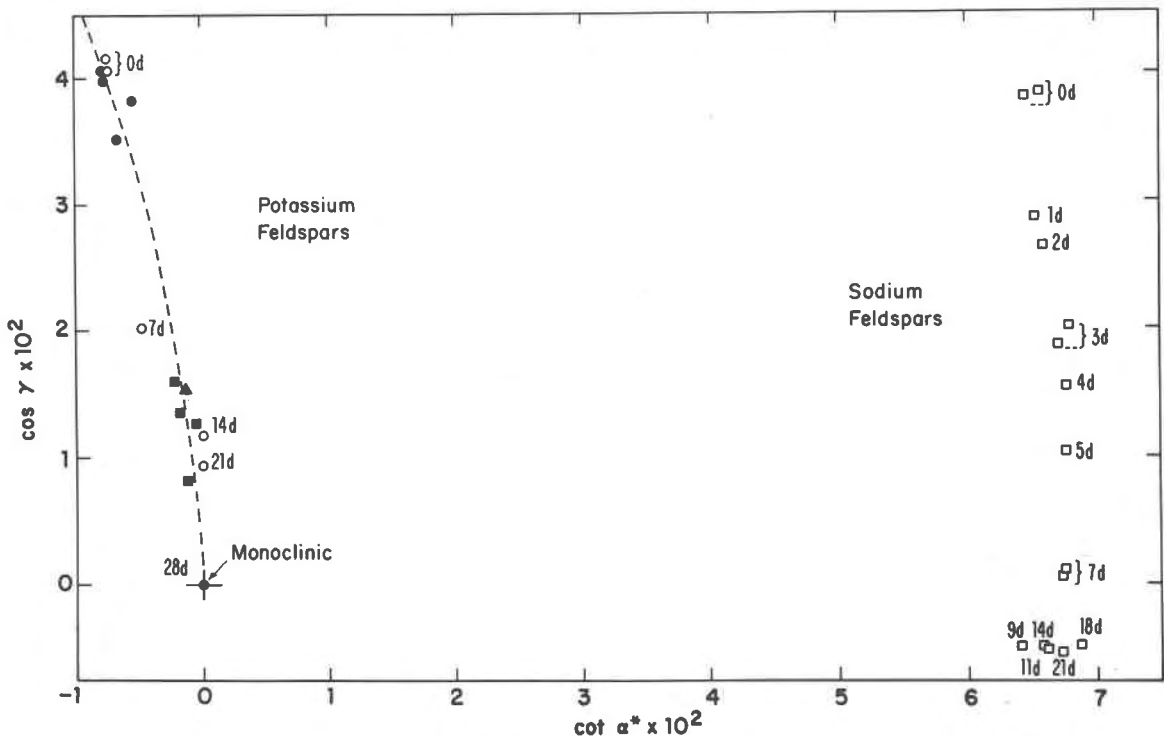


Fig. 3. Angular relations in some end-member alkali feldspars: Open circles are heated authigenic microcline (Baskin, 1956), numbers show number of days heated at  $\sim 1100^\circ\text{C}$ ; open squares are corresponding data (Baskin, 1956) for a low albite from Switzerland; solid circles are authigenic microclines (Kastner, 1971); solid squares are intermediate microclines of Wright and Stewart (1968); solid triangle is the intermediate microcline of Bailey and Taylor (1955). All observations at room temperature.

have highly ordered Al-Si distributions and that the high-temperature forms have highly disordered Al-Si distributions. The principal effect of Al-Si ordering is thus to increase the obliquity of the (001) face of the unit cell.

Because ordering or disordering of the Al and Si atoms is a slow process, the effects of short-term heating experiments are essentially reversible in that the room-temperature properties in many instances remain virtually unaltered. High-temperature X-ray studies show that K-feldspars experience only negligible variation (Grundy and Brown, 1967) in  $\alpha^*$  and  $\gamma$  on heating, but that Na-feldspars (Grundy and Brown, 1969; Stewart and von Limbach, 1967) and Ca-feldspars (Grundy and Brown, 1967, 1974) experience a marked decrease in  $\cot\alpha^*$  accompanied by relatively minor changes in  $\cos\gamma$ . The results for Na- and Ca-feldspars are shown in Figure 4. The sequence for one of the feldspars is also shown separately in Figure 5 in order to demonstrate graphically

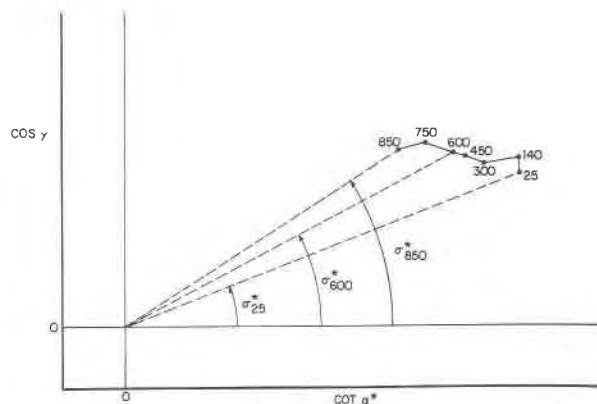


Fig. 5. Changes in  $\sigma^*$  and  $\phi$  with temperature for an intermediate albite (219 of Grundy and Brown, 1969). Lengths of the dashed lines are very nearly equal to the corresponding magnitudes of  $\phi$  (in radians), as explained in the text.

the effect on  $\sigma^*$  and  $\phi$ . Because these changes are rapid and reversible, the structural changes associated with them are clearly displacive rather than diffusive, as was first pointed out by Laves (1952).

The quantity  $(1 - \cos\phi)$  must vanish if a feldspar becomes monoclinic, or dimensionally so, and it is an even-symmetric property in the sense of Thompson *et al.* (1974). It may thus be used to aid in locating triclinic-monoclinic transformations in various feldspar series. In Figure 6 this quantity is plotted as a function of temperature for an analbite (MacKenzie, 1957; Grundy and Brown, 1969) and also for an anorthite (Grundy and Brown, 1967). This albite is monoclinic at 950°C. The line fitted to the anorthite points has the equation<sup>1</sup>

<sup>1</sup> The number in parentheses represents the estimated standard deviation of the least significant figure quoted.

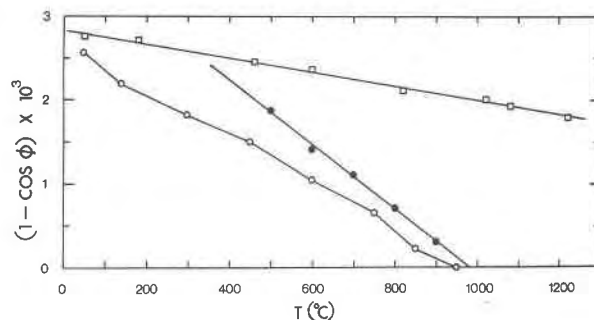


Fig. 6. Variations of  $(1 - \cos\phi)$  with temperature: open circles are analbite (307 of Grundy and Brown, 1969); closed circles are "equilibrated" albites at temperature of equilibration (Grundy and Brown, 1969); open squares are anorthite (F72 of Grundy and Brown, 1967). Lines through the anorthite and albite points correspond to equations (26) and (30), respectively.

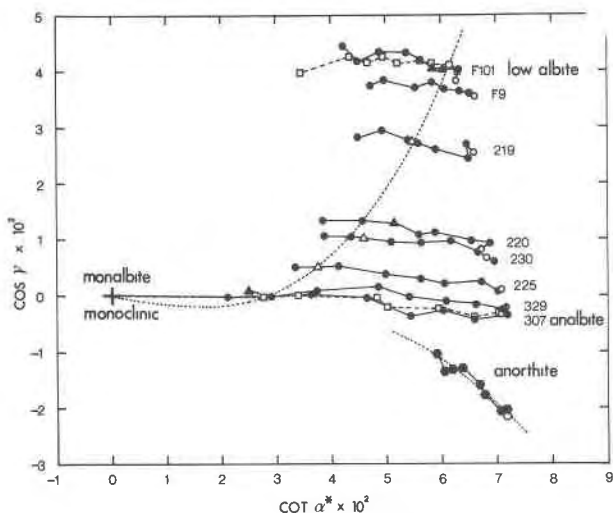


Fig. 4. Results of short-term heating of Na- and Ca-feldspars. Circles (numbered series) are albites of MacKenzie (1957) and Grundy and Brown (1969); open circles are room-temperature measurements after heating, closed circles for all series except F9 from right to left represent measurements at temperatures of 25°, 140°, 300°, 450°, 600°, 750°, and 850°C. In addition, series F101 and 307 have data points at 950°, and series 329 has a data point at 900°C. Triangles are data for "equilibrated" albites at the temperatures of equilibration. Open squares are corresponding data from Stewart and von Limbach (1967), temperatures of the measurements increasing from right to left. Hexagons are for the F72 anorthite series of Grundy and Brown (1967), temperatures increasing from lower right to upper left. The open hexagon represents a room-temperature measurement after heating. Dashed curves through the "equilibrated" albites and through the anorthite series represent relations given by equations (29) and (28), respectively.

$$(1 - \cos\phi) = 0.002820(10) - 8.27(13) \times 10^{-7}T(^{\circ}\text{C}) \quad (26)$$

hence it is evident that this feldspar could only become monoclinic if superheated well above its melting point.

**Alkali-exchange series**

Short-term alkali-exchange experiments (Orville, 1967; Wright and Stewart, 1968), like short-term heating experiments, leave the Al-Si distribution virtually unaltered, hence are essentially reversible. Several such series for Ca-free feldspars are shown in Figure 7, as observed at room temperature. Comparison with Figure 4 shows that the effect of replacing Na by K on  $\alpha^*$  and  $\gamma$  is very much the same as that of short-term heating at constant composition. Certain highly disordered alkali feldspars may thus be converted into monoclinic forms either by heating or by exchange of K for Na. Similar results have been obtained by Kroll and Bambauer (1971) by exchanging K for Na in calcic feldspars. High-temperature plagioclases more sodic than  $\text{An}_{50}$  may be converted into monoclinic forms by this process followed by short-term heating. If barium could be exchanged for calcium it is possible that some of the highly calcic plagioclases could also be converted to monoclinic forms, inasmuch as their Al-Si distributions are consistent with it (Megaw *et al.*, 1962) or very nearly so.

**Plagioclase feldspars**

The results of Grundy and Brown (1967, 1974), some of which have been plotted in Figure 8, show that plagioclases less calcic than  $\text{An}_{75}$  behave like Na-feldspars in the contrast between the effects of short-

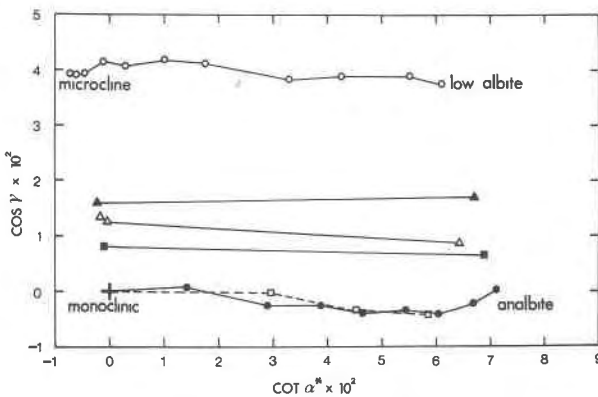


Fig. 7. Alkali-exchange series: circles (solid, analbite-sandine; open, low albite-microcline) from Orville (1967); open squares (analbite-orthoclase), solid triangles (Albite III), open triangles (Spencer U), and solid squares (S62-34) from Wright and Stewart (1968).

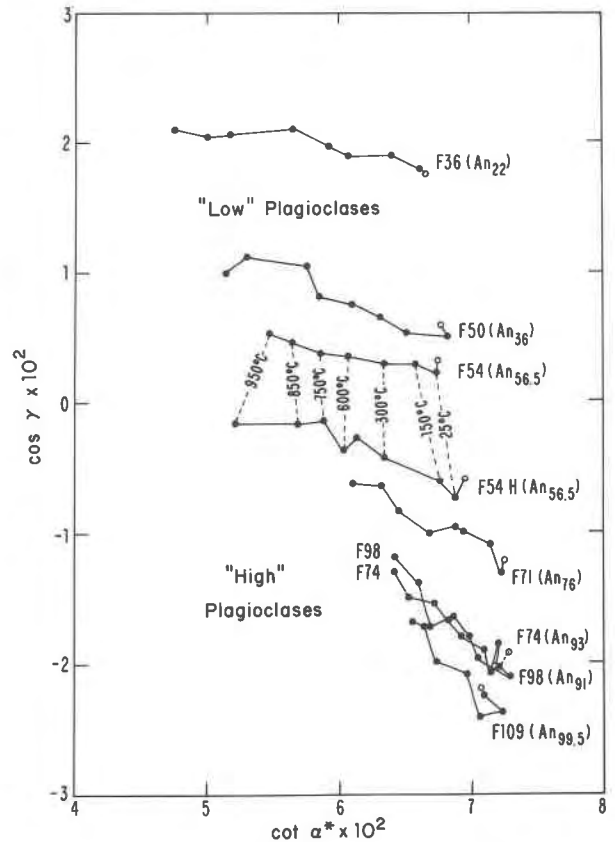


Fig. 8. Short-term and long-term heating of plagioclases (all data from Grundy and Brown, 1974). Sample F54H was prepared by long-term heat treatment (7 days, 1080°C) of sample F54.

term and long-term heating experiments. More calcic plagioclases, however, show only the short-term effects.

**Equilibrated feldspars**

For feldspars that are fully equilibrated internally, there should be a unique value of  $\alpha^*$  and  $\gamma$  for each pressure, temperature, and composition. It thus follows that for each feldspar composition there should be a unique path in terms of  $\alpha^*$  and  $\gamma$  or their trigonometric functions. For pure K-feldspars, which show only the diffusive changes, and for pure Ca-feldspars, which show only the displacive ones, these paths must be essentially the ones shown by dashed lines in Figures 3 and 4. For the K-feldspars the path may be formulated, tentatively, as

$$\cot\alpha^* = -0.095(7) \cos\gamma - 56(7) \cos^3\gamma \quad (27)$$

and for the Ca-feldspars as

$$\cos\gamma = 0.046(17) \cot\alpha^* - 66(4) \cot^3\alpha^* \quad (28)$$



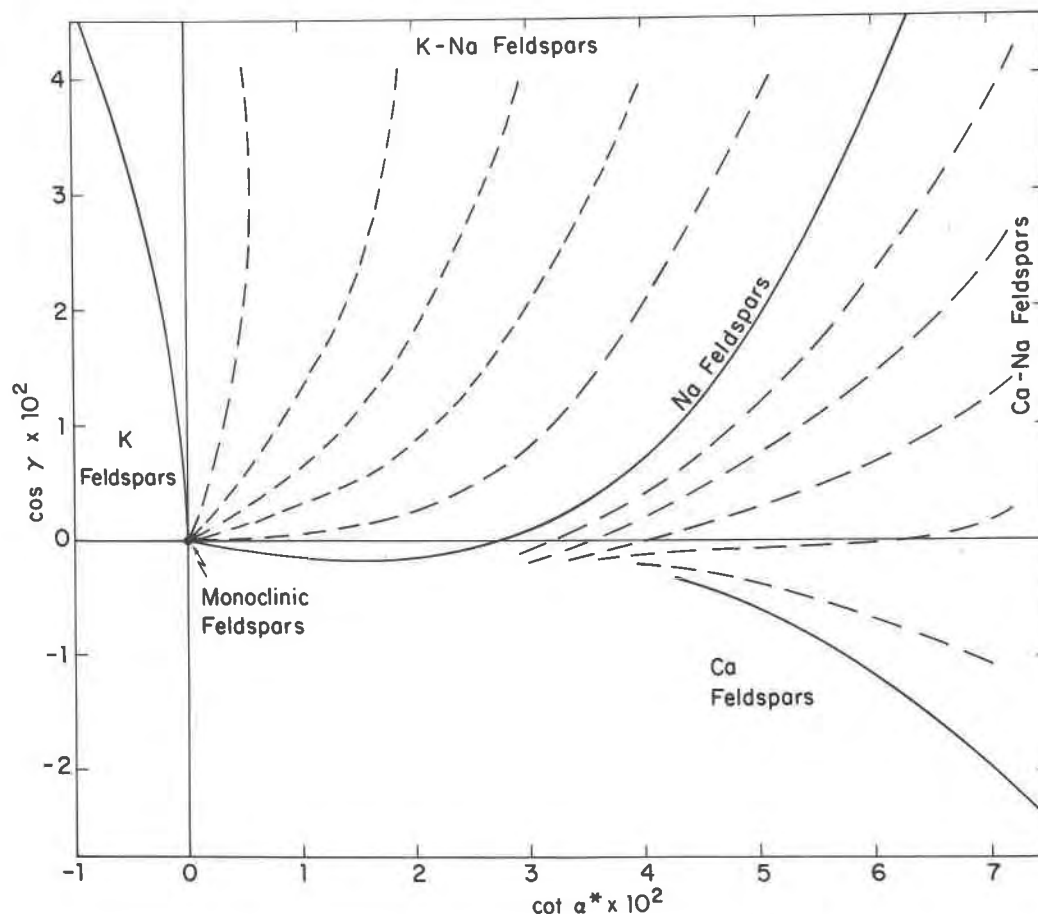


Fig. 9.  $\alpha^*$ - $\gamma$  paths for equilibrated K-Na-Ca feldspars. Solid curves correspond to equations (27), (28) and (29), dashed ones are schematic for K-Na and Na-Ca feldspars.

Pure Na-feldspars, however, are more complex because they show both the displacive and diffusive effects, hence cover a wide area in a plot such as that of Figure 4, rather than having a distribution that may be approximated by a simple plane curve. Certain of the feldspars in Figure 4, however, were synthesized originally by MacKenzie (1957) and held at temperature until any observable variation in their crystallographic properties became negligible. They are, therefore, probably near the true equilibrium albites for their temperatures of synthesis. The observed (solid triangles) or interpolated (open triangles) values of  $\cot\alpha^*$  and  $\cos\gamma$  for these feldspars are shown in Figure 4, and the curve passing through them has the equation

$$\cos\gamma = -0.10(6) \cot\alpha^* + 166(26) \cot^3\alpha^* \quad (29)$$

The solid circles in Figure 6 correspond to the triangles in Figure 4, and the dashed line passing through them has the equation

$$(1 - \cos\phi) = 0.00376(6) - 3.82(8) \times 10^{-6} T(^{\circ}\text{C}) \quad (30)$$

indicating that the temperature of the triclinic-monoclinic transformation for fully equilibrated albites is close to 983°C (compare with Thompson *et al.*, 1974, Fig. 9).

Equations (26) and (28) thus constitute a preliminary formulation of the angular properties of equilibrated Ca-feldspars as functions of each other and temperature, and equations (29) and (30) do the same for equilibrated Na-feldspars. For K-feldspars we have only equation (27), owing to the lack of known equilibration temperatures for the various triclinic K-feldspars.

The general form of the probable paths for equilibrated K-Na-Ca feldspars is shown in Figure 9. The solid curves are for the end-member feldspars as based on equations (27), (28), and (29). The dashed curves are schematic and are presented to encourage others to obtain a better set.

### Acknowledgments

The computational expenses for this investigation were met by NSF grant EAR 75-21852, and by the Higgins Fund of Harvard University. We are grateful to G. E. Brown and H. R. Wenk for their helpful comments on the manuscript, and to Clifford Frondel and Cornelius Hurlbut for the many years we have known them as colleagues and teachers, and for their cheerful assistance at various stages of our feldspar investigations.

### References

- Bailey, S. W. and W. H. Taylor (1955) The structure of a triclinic potassium feldspar. *Acta Crystallogr.*, **8**, 621–632.
- Baskin, I. (1956) Observations on heat-treated authigenic microcline and albite crystals. *J. Geol.*, **64**, 214–224.
- Cole, W. F., H. Sörum and W. H. Taylor (1951) The structure of the plagioclase feldspars, I. *Acta Crystallogr.*, **4**, 20–29.
- Donnay, J. D. H. (1940) Width of albite-twinning lamellae. *Am. Mineral.*, **25**, 578–586.
- Gay, P. (1956) A note on albite twinning in plagioclase feldspars. *Mineral. Mag.*, **31**, 301–305.
- Goldsmith, J. R. and F. Laves (1954) The microcline–sanidine stability relations. *Geochim. Cosmochim. Acta*, **5**, 1–19.
- Grove, T. L. and R. M. Hazen (1974) Alkali feldspar unit-cell parameters at liquid nitrogen temperatures: low temperature limits of the displacive transformation. *Am. Mineral.*, **59**, 1327–1329.
- Grundy, H. D. and W. L. Brown (1967) Preliminary single-crystal study of the lattice angles of triclinic feldspars at temperatures up to 1700°. *Schweiz. Mineral. Petrogr. Mitt.*, **47**, 21–30.
- and ——— (1969) A high-temperature X-ray study of the equilibrium forms of albite. *Mineral. Mag.*, **37**, 156–172.
- and ——— (1974) A high-temperature X-ray study of low and high plagioclase feldspars. In W. S. MacKenzie and J. Zussman, Eds., *The Feldspars*, p. 162–173. University Press, Manchester.
- Kastner, M. (1971) Authigenic feldspars in carbonate rocks. *Am. Mineral.*, **56**, 1403–1442.
- Kroll, H. and H. U. Bambauer (1971) The displacive transformation of (K,Na,Ca) feldspars. *Neues Jahrb. Mineral. Monatsh.*, **413–416**.
- Laves, F. (1951) A revised orientation of microcline and its geometrical relation to albite and cryptoperthites. *J. Geol.*, **59**, 510–511.
- (1952) Phase relations of the alkali feldspars. I Introductory remarks. *J. Geol.*, **60**, 436–450.
- Lewis, W. J. (1899) *A Treatise on Crystallography*. Cambridge University Press, Cambridge, England.
- MacKenzie, W. S. (1957) The crystalline modifications of  $\text{NaAlSi}_3\text{O}_8$ . *Am. J. Sci.*, **255**, 481–516.
- and J. V. Smith (1955) The alkali feldspars. I. Orthoclase–microperthites. *Am. Mineral.*, **40**, 707–732.
- Martin, R. F. (1969) The hydrothermal synthesis of low albite. *Contrib. Mineral. Petrol.*, **23**, 323–339.
- (1970) Cell-parameters and infrared absorption of synthetic high to low albites. *Contrib. Mineral. Petrol.*, **26**, 62–74.
- McConnell, J. D. C. and D. McKie (1960) The kinetics of the ordering process in triclinic  $\text{NaAlSi}_3\text{O}_8$ . *Mineral. Mag.*, **32**, 436–454.
- Megaw, H. D., C. J. E. Kempster and E. W. Radoslovich (1962) The structure of anorthite,  $\text{CaAl}_2\text{Si}_2\text{O}_8$ , II. Description and discussion. *Acta Crystallogr.*, **15**, 1017–1035.
- Mügge, O. (1930) Ueber die Lage des rhombischen Schnittes im Anorthit und seine Bedeutung als geologisches Thermometer. *Z. Kristallogr.*, **75**, 337–344.
- Orville, P. M. (1967) Unit-cell parameters of the microcline–low albite and the sanidine–high albite solid solution series. *Am. Mineral.*, **52**, 55–86.
- Rath, G. vom (1876) Die Zwillingverwachsung der triklinen Feldspathe nach dem sog. Periklin-Gesetz und über eine darauf gegründete Unterscheidung derselben. *Neues Jahrb. Mineral.*, **1876**, 689–715.
- Rosenbusch, H. and O. Mügge (1927) *Mikroskopische Physiographie der Mineralien und Gesteine. Bd. 1, Zweite Hälfte: Die petrographisch wichtigen Mineralien, Spezieller Teil*. Schweizerbart'sche Verlagsbuchhandlung, Stuttgart.
- Stewart, D. B. and D. von Limbach (1967) Thermal expansion of low and high albite. *Am. J. Sci.*, **267A**, 44–62.
- Story-Maskelyne, N. (1895) *Crystallography*. Oxford University Press, Oxford, England.
- Thompson, J. B., D. R. Waldbaum and G. L. Hovis (1974) Thermodynamic properties related to ordering in end-member alkali feldspars. In W. S. MacKenzie and J. Zussman, Eds., *The Feldspars*, p. 218–248. Manchester University Press, Manchester, England.
- Tunell, G. (1952) The angle between the *a*-axis and the trace of the rhombic section on the (010)-pinacoid in the plagioclases. *Am. J. Sci.*, (Bowen Vol.), **547–551**.
- Wright, T. L. and D. B. Stewart (1968) X-ray and optical study of alkali-feldspars. I. Determination of composition and structural state from refined unit-cell parameters and 2V. *Am. Mineral.*, **53**, 38–87.

Manuscript received, April 3, 1978; accepted for publication, June 6, 1978.